Physiological Reports

Open Access

Physiological Reports ISSN 2051-817X

ORIGINAL RESEARCH

Maxi-K channel (BK_{Ca}) activity veils the myogenic tone of mesenteric artery in rats

Eun Yeong Suh[1], Ming Zhe Yin[1], Haiyue Lin[1], Yin Hua Zhang[1], Hae Young Yoo[2] & Sung Joon Kim[1]

1 Departments of Physiology and of Biomedical Sciences, Seoul National University College of Medicine, Seoul, Korea
2 Chung-Ang University Red Cross College of Nursing, Seoul, Korea

Keywords
BK_{Ca}, K^+ channel, mesenteric artery, myogenic tone, vascular smooth muscle cell.

Correspondence
Sung Joon Kim
Departments of Physiology and Biomedical Sciences, Seoul National University College of Medicine, Seoul, Korea.
Tel: +82-2-740-8230
Fax: +82-2-763-9667
E-mail: sjoonkim@snu.ac.kr

Funding Information
This work was supported by a National Research Foundation of Korea (NRF) grant funded by the Korea government (MSIP) (no. 2007-0056092 and 2011-0017370) and the Seoul National University Hospital.

Received: 25 January 2017; Revised: 30 May 2017; Accepted: 31 May 2017

doi: 10.14814/phy2.13330

Physiol Rep, 5 (14), 2017, e13330, https://doi.org/10.14814/phy2.13330

Abstract

Arterioles and small arteries change their tone in response to transmural pressure changes, called myogenic tone (MT). In comparison to the branches of cerebral arteries (CA) showing prominent MT, the third branches of mesenteric arteries (MA) with similar diameters show weaker MT. Here, we aimed to analyze the electrophysiological differences responsible for the weaker MT in MA (MT_{MA}) than MT in CA (MT_{CA}). We measured ionic current using patch clamp in isolated MA smooth muscle cells (MASMCs) and CA smooth muscle cells (CASMCs) of rats. MT was analyzed using video analysis of pressurized small arteries. Quantitative-PCR (q-PCR) and immunofluorescence confocal microscopy were used to compare the mRNA and protein expression level of big-conductance Ca^{2+}-activated K^+ channel (BK_{Ca}) subunits (Slo1α and Sloβ1). Whole-cell patch clamp study revealed higher density of voltage-operated Ca^{2+} channel current (I_{CaV}) in the MASMCs than in CASMCs. Although voltage-gated K^+ channel current (I_{Kv}) was also higher in MASMCs, treatment with Kv inhibitor (4-aminopyridine) did not affect MT_{MA}. Interestingly, BK_{Ca} current density and the frequency of spontaneous transient outward currents (STOCs) were consistently higher in MASMCs than in CASMCs. Inside-out patch clamp showed that the Ca^{2+}-sensitivity of BK_{Ca} is higher in MASMCs than in CASMCs. Iberiotoxin, a selective BK_{Ca} inhibitor, augmented MT_{MA} by a larger extent than MT_{CA}. Although q-PCR analysis did not reveal a significant difference of mRNAs for Slo1α and Sloβ1, immunofluorescence image suggested higher expression of Slo1α in MASMCs than in CASMCs. Despite the large I_{CaV} density, the high activities of BK_{Ca} including the more frequent STOCs in MASMCs veils the potentially strong MT_{MA}.

Introduction

Small arteries and arterioles show contractile responses to an increase in luminal pressure (P_{lum}). Since the contraction occurs independent of neurohumoral influences, it is named as myogenic tone (MT) of arteries. MT contributes to the peripheral resistance of vascular system, and thus blood pressure (Hill et al. 2006). Also, MT enables fine regulation of arterial diameter for constant regional blood flow despite the fluctuation of perfusion pressure, called autoregulation (Johnson 1977). The autoregulation of blood flow is observed in various organs such as brain and kidney. Among various types of vessels, cerebral arteries (CA) has been intensely investigated with regard to the mechanisms and pathophysiological implication of MT, reflecting physiological importance of autoregulation in the cerebral blood flow (Cipolla et al. 2014). Skeletal arteries such as cremaster artery and deep femoral artery also show robust MT (Kotecha and Hill 2005; Baek et al. 2010).

In the intestinal circulation, mesenteric arterial branches pierce the muscle layer to form microcirculatory networks in submucosa. It was reported that major part of the pressure drop in the intestine occurs in the precapillary arterioles. However, a significant pressure drop in the mesenteric arteries (MA) has indicated that MAs are

not simple conduit but have active control of resistance (Lundgren 1989). In fact, previous studies have shown that the small branches of MA show MT (Sun et al. 1992; Enouri et al. 2011). Nevertheless, a closer inspection of literature reveals that the MT of MA (MT_{MA}) is less consistent in the absence of agonists (VanBavel et al. 1991; Chlopicki et al. 2001; Mathewson and Dunn 2014). Also, MT_{MA} appears to be lower than the MT of CA (MT_{CA}) and of skeletal arteries (Lagaud et al. 1999, 2002; Baek et al. 2010).

The relatively low MT_{MA} might be due to weak mechanosensation or effector functions in the mesenteric arterial smooth muscle cells (MASMCs). Since the wall tension changes induced by the increased luminal pressure (P_{lum}) is accompanied by membrane depolarization and activation of voltage-gated Ca^{2+} channels (CaV) in the smooth muscle cells (Harder 1984; Wesselman et al. 1996), differential activities of CaV might be responsible for the different levels of MT. Another plausible difference might be the activities of K^+ channels; hyperpolarizing influence from K^+ channels would attenuate MT via antagonizing inward cationic conductances including CaV. Voltage-gated K^+ channels (Kv) and big-conductance Ca^{2+}-activated K^+ channel (BK_{Ca}) are commonly expressed in the most types of arterial myocytes (Standen and Quayle 1998). In addition, inwardly rectifying K^+ channels (Kir) also play important roles in the fine regulation of resistance arteries including CA. However, the expression of Kir is not significant in MASMCs (Smith et al. 2008; Jin et al. 2011; Sonkusare et al. 2016).

The density of BK_{Ca} current and the expression of corresponding proteins (Slo1) are generally higher in smooth muscle cells than other cell types (Hu and Zhang 2012). BK_{Ca} are concertedly activated by increased cytosolic Ca^{2+} concentration ($[Ca^{2+}]_c$) and membrane depolarization. BK_{Ca} activity not only reflects the overall $[Ca^{2+}]_c$, but also the dynamic changes of subsarcolemmal concentration $[Ca^{2+}]_{sl}$. From the early period of patch clamp studies in both visceral and vascular smooth muscle cells, spontaneous transient outward currents (STOCs) lasting about 100 msec have been observed under physiological intracellular Ca^{2+} buffering conditions. The STOCs are thought to represent the simultaneous opening of up to a hundred BK_{Ca} (Benham and Bolton 1986) . Combined with $[Ca^{2+}]_c$ measurement studies, STOCs are generally accepted to reflect localized events of strong increase in the $[Ca^{2+}]_{sl}$, called Ca^{2+} sparks (Bolton and Imaizumi 1996). The hyperpolarizing influence of averaged STOCs contributes to the level of the arterial tone via setting the membrane potential (Pérez et al. 1999). Thus, comparative analysis of BK_{Ca} and their roles between different arteries are worth investigating to understand the functional differences between vessels (Hill et al. 2010). A previous study showed higher Ca^{2+} sensitivity of BK_{Ca} and higher expression of Slo-1 beta subunit in cerebral arterial myocytes (CASMCs) than skeletal arterial smooth muscle cells (SkASMCs) (Yang et al. 2013). Even between the CA branches, the relatively large pial arteries show more influential role of BK_{Ca} than the smaller parenchymal arteries (Cipolla et al. 2014). However, the comparative study of BK_{Ca} in MASMCs with other arterial myocytes is lacking, especially related with the differential levels of MT.

On these backgrounds, here we investigate the activities of CaV, Kv, and BK_{Ca} currents in MASMCs and CASMCs. Along with the electrophysiological data, effective augmentation of smaller MT_{MA} by BK_{Ca} inhibitor suggest that higher activities of BK_{Ca} in MASMCs than CASMCs exert prominent auto-inhibitory effect on MA.

Materials and Methods

Experimental animals

Male Sprague–Dawley (S–D) rats (8 weeks old) were fully anesthetized with pentobarbital sodium (100 mg/kg ip) and immediately sacrificed by decapitation. And their brain and gastrointestinal tract with mesentery arcade were moved into a normal Tyrode's (NT) solution. The study protocol was in accordance with the Guide for the Care and Use of Laboratory Animals published by the US National Institutes of Health (NIH Publication Eighth edition, revised 2011), and also conforms to the Institutional Animal Care and Use Committee (IACUC) in Seoul National University (IACUC approval No.: SNU-111214-4-1)

Measurement of vascular myogenic tone in resistance arteries

The third and fourth-order branches of mesenteric arteries and the first-branches of posterior and cerebellar arteries (200–250 μm) were carefully dissected under the stereomicroscope. The arterial segments were placed in a glass-bottomed vessel chamber (Model CH/1/SH; Living Systems Instrumentation, Burlington, VT). The vessel chamber contained NT and its composition was as follows (in mmol/L): 141.4 NaCl, 4 KCl, 1 $MgCl_2$, 1.8 $CaCl_2$, 0.33 NaH_2PO_4, 10 Glucose, and 10 HEPES (4-(2-hydroxyethyl)-1-piperazineethanesulfonic acid), adjusted to pH 7.4 with NaOH. The temperature was set at 37–38°C using a controller (Model TC-01; Living Systems Instrumentation). The vessels were cannulated using glass micropipettes and secured with 12–0 nylon suture. Inner diameters (D_{in}) of pressurized vessels were measured using a UBS CCD camera (DMK 41AU02, The Imaging

Source, Bremen, Germany) and DMTVAS 6.2 software (IonOptix LLC, Milton, MA, USA). The value of luminal pressure (P_{lum}) was set to 60 mmHg for at least an additional 40 min; spontaneous tone (i.e., decrease in vessel diameter) developed within this time frame and reached a steady state. Arterial segments without stable tone were discarded. After confirming the generation of myogenic tone, P_{lum} was lowered to 30 mmHg and incubated for equilibrium, the increase to 60 and 100 mmHg evaluate the MT. On the step-like increase in P_{lum}, D_{in} initially increased and then slowly decreased. To quantify MT of arteries, the maximal passive diameter ($D_{max,0Ca}$) was measured in Ca^{2+}-free NT solution (0Ca-NT) with 1 mmol/L EGTA (ethylene glycol-bis(2-aminoethylether)-N,N,N′,N′-tetraacetic acid). The maximal increase in D_{in} (ΔD_{max}) by changing to the 0Ca-NT was divided by $D_{max,0Ca}$ ($\Delta D_{max}/D_{max,0Ca}$), resulting the MT (%) at each P_{lum}.

Vascular smooth muscle cell isolation

After the dissection of arteries, vessels were initially incubated in 1 mL of the digestion medium I (0Ca-NT solution containing 1 mg/mL papain) for 10–15 min and changed to the digestion medium II (0Ca-NT solution containing 3 mg/mL collagenase) for another 10–15 min. Both digestion media contained bovine serum albumin (1 mg/mL) and dithiothreitol (1 mg/mL). The enzyme-treated arteries were then gently agitated using a fire-polished glass pipette and in a K^+-rich solution modified from KB solution (Isenberg and Klockner 1982), that contained (in mmol/L): 70 KOH, 50 L-glutamate, 55 KCl, 20 taurine, 20 KH_2PO_4, 3 $MgCl_2$, 20 Glucose, 10 HEPES, and 0.5 EGTA, adjusted to pH 7.3 with KOH.

Electrophysiological recording

Isolated cells were transferred to a small chamber (0.2 mL) on the stage of an inverted microscope (IX-70; Olympus, Osaka, Japan). The conventional whole-cell or inside-out configuration was performed with a patch-clamp amplifier (Axopatch-1C; Axon Instruments, Foster City, CA) and voltage-clamp experiments were performed at room temperature (22–25°C). Membrane currents were recorded using the glass microelectrode with a resistance of 2–2.5 MΩ and 7–8 MΩ for whole-cell and inside-out patch clamp recordings, respectively. The signals were filtered at 5.0 kHz and sampled at a rate of 2.0 kHz and 10.0 kHz for whole-cell and inside-out patch clamp recordings, respectively. The pCLAMP software v.9.2 and Digidata-1440A (Axon Instruments) were used to acquire data and apply command pulses.

The name and composition of the experimental solutions used in the electrophysiological recording are as below. The bath solution for recording CaV (whole-cell) current contained the following (in mmol/L): 120 NaCl, 5 CsCl, 10 HEPES, 10 Glucose, 10 $BaCl_2$, 10 tetraethylammonium chloride (TEA-Cl), 0.5 $MgCl_2$, adjusted to pH 7.4 with NaOH. The pipette solution for recording the CaV current contained (in mmol/L): 20 CsCl, 10 HEPES, 1 $MgCl_2$, 5 EGTA, 120 Aspartic acid (Asp), 3 Mg-ATP, adjusted to pH 7.2 with CsOH. To record the Kv current (whole-cell), the NT solution contained 1 mmol/L TEA was used as bath solution. The pipette solution for recording the Kv contained the following (in mmol/L): 20 KCl, 10 HEPES, 1 $MgCl_2$, 5 EGTA, 120 Asp, 3 Mg-ATP, adjusted to pH 7.2 with KOH. To investigate the BK_{Ca} current (whole-cell), we used the NT as bath solution. The pipette solution contained (in mmol/L): 20 KCl, 10 HEPES, 1 $MgCl_2$, 120 Asp, 3 Mg-ATP; pH was adjusted to 7.2 with KOH. And free Ca^{2+} activity in the pipette solution was clamped to 1 μmol/L using 10 mmol/L EGTA and $CaCl_2$ with WinMAX program (Chris Patton, Stanford University, http://www.stanford.edu/~cpatton/maxc.html). For recording STOCs (whole-cell), we used the NT as bath solution. The pipette solution contained (in mmol/L): 20 KCl, 10 HEPES, 1 $MgCl_2$, 0.1 EGTA, 120 Asp, 3 Mg-ATP; pH was adjusted to 7.2 with KOH. To analyze the single-channel conductance of BK_{Ca} (inside-out), the bath solution contained the following (in mmol/L): 140 KCl, 10 HEPES, 10 Glucose, 1 $MgCl_2$; pH was adjusted to 7.2 with KOH. And we added 10 mmol/L EGTA and $CaCl_2$ in the bath solution to fix at 1 μmol/L free Ca^{2+}. The pipette solution contained the following (in mmol/L): 140 KCl, 10 HEPES, 10 Glucose, 1 $MgCl_2$; pH was adjusted to 7.4 with KOH. To investigate Ca^{2+}-dependent activation of BK_{Ca} (inside-out), the bath solution contained (in mmol/L): 140 KCl, 10 HEPES, 10 Glucose, 1 $MgCl_2$, adjusted pH to 7.2 with KOH; variable amounts of $CaCl_2$ were added to the bath solution to obtain 3, 10, and 30 μmol/L free Ca^{2+}. We made 3 and 10 μmol/L free Ca^{2+} solution using 10 mmol/L of N-(2-Hydroxyethyl) ethylenediamine-N,N′, N′-triacetic acid (HEDTA) and $CaCl_2$ calculated with the WinMAX program. For making 30 μmol/L free Ca^{2+} solution, we simply added $CaCl_2$ to the bath solution. We used NT as pipette solution.

Real-time quantitative PCR

Total RNA was extracted using TRizol reagent (Invitrogen), and its purified concentration was determined NanoDrop at 260 nm. The extracted RNA was reverse transcripted into cDNA using the PrimeScript RT Master Mix Perfect Real Time (Takara) according to the manufacturer's instructions. The cDNA was amplified using the primers as follows: GAPDH (forward, 5′-

ACGGCAAATTCAACGGCACAGTCA; reverse, 5′-TGGG GGCATCGGCAGAAGG; BK_{Ca} α-subunit (Slo1α, forward, 5′-AAACAAGTAATTCCATCAAGCTGGTG; reverse, 5′-CGTAAGTGCCTGGTTGTTTTGG); BK_{Ca} β1-subunit (Sloβ1, forward, 5′-GTCTGCATCTTTGGGGATGT; reverse, 5′-GGGGAAGGTGTGCAGTGTTT). cDNAs were amplified with SYBR Green (TOPreal qPCR 23 PreMIX) using a real-time PCR system (Applied Biosystems 7500 real-time PCR) under the conditions 95°C for 10 min, 40 cycles at 95°C for 10 sec, 55°C for 15 sec, and 72°C for 20 sec. After the final PCR cycle, a melting curve analysis was performed to analyze the specificity of the reaction. Relative gene expression was calculated using the comparative threshold (Ct) method ($2^{-\Delta\Delta Ct}$).

Immunofluorescence confocal microscopy

Fresh isolated MASCMs and CASMCs were fixed with 4% paraformaldehyde for 30 min and permeabilized with 0.1% Triton X-100 for 15 min at room temperature. Then

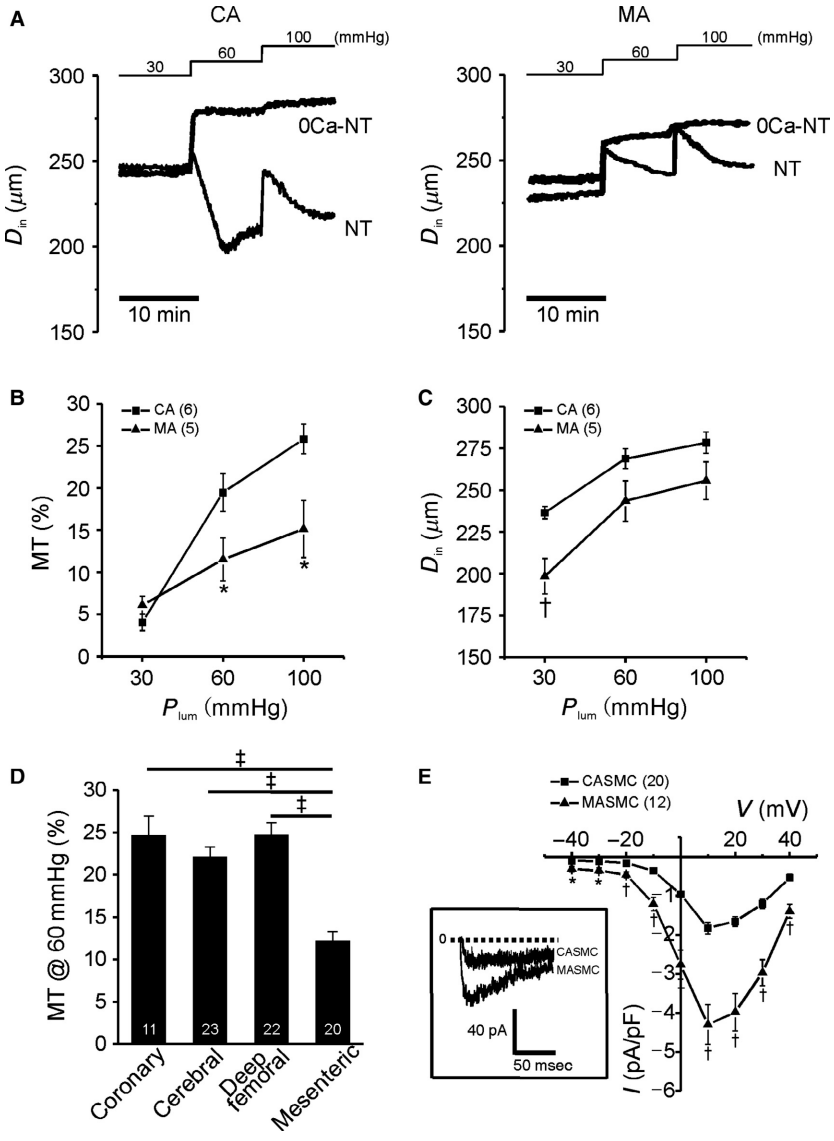

Figure 1. Low myogenic tone in MA despite relatively high I_{CaV} in MASMCs. (A) Representative traces of D_{in} change in response to stepwise increase in P_{lum} (left; CA, right; MA). (B) Myogenic tone normalized to maximal passive D_{in} ($D_{max,0Ca}$) from CA and MA (*$P < 0.05$). (C) Summary of the $D_{max,0Ca}$ recorded in Ca^{2+} free condition (0Ca-NT) ($^{\dagger}P < 0.01$). (D) Comparison of myogenic tone at 60 mmHg in different type of arteries (coronary, cerebral, deep femoral, mesenteric) ($^{\ddagger}P < 0.001$). (E) Summary of nifedipine-sensitive I_{CaV} in CASMCs and MASMCs (*$P < 0.05$). Representative recording at depolarizing membrane voltage (+10 mV) obtained by Cs^{+}-rich pipette and Ba^{2+} containing NT bath solution was shown in the inset (left panel of E) (*$P < 0.05$).

cells were blocked with 10% FBS for 1 h at room temperature, and incubated with primary antibodies of anti-Slo1α-subunit (1:50 diluted in 5% FBS, Alomone labs) or anti-Sloβ1-subunit (1:200 diluted in 5% FBS, Abcam) overnight at 4°C. The channels expression levels were detected using Alexa Fluor 488-conjugated goat anti-rabbit secondary antibody (1:500 diluted with 5% FBS, Invitrogen). Imaged were acquired with Olympus FV1000 confocal microscope with a ×100 oil immersion objective.

Drugs and chemicals

All drugs and chemicals used in this study were purchased from Sigma Chemical Co. (St Louis, MO) excluding iberiotoxin. Iberiotoxin was purchased from Tocris (Ellisville, MO).

Statistical analysis

Data are shown as means ± SEM with the number of tested arteries indicated as *n*. Student's unpaired t-test was used to test for significance at the level of 0.05.

Results

Representative traces of CA and D_{in} during the step-like increase P_{lum} from 30 to 60 and 100 mmHg showed rebound contractions following initial passive dilation, consistent with the presence of MT (Fig. 1A). In the 0Ca-NT, only the passive dilation was commonly observed on the P_{lum} increase (Fig. 1A). The MT_{MA} was significantly smaller than MT_{CA} (Fig. 1B). It was notable that the passive diameters of MA (3rd and 4th branches) used in this study were generally smaller than those of CA, especially at 30 mmHg of P_{lum} (Fig. 1C, Ca^{2+}-free condition). We also compared MT_{MA} with the MT of coronary and deep femoral arteries; MT_{MA} was consistently lower than the MT from the other types of arteries (Fig. 1D).

I_{CaV} was analyzed in MASMCs and CASMCs using the whole-cell patch-clamp technique using CsCl pipette solution. Step-like depolarizations were applied from −70 mV of holding voltage, which revealed voltage-dependent activation of inward currents (Fig. 1E, inset). Peak amplitudes of I_{CaV} versus recording voltages were plotted (*I*/*V*

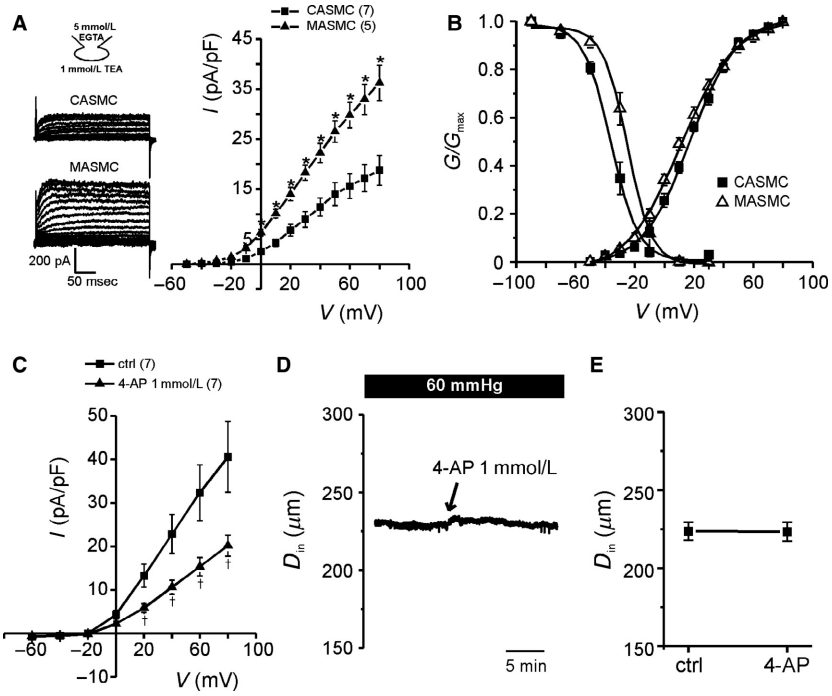

Figure 2. Higher amplitudes of I_{Kv} in MASMCs than CASMCs. (A) Left: representative Kv current recorded in CASMCs and MASMCs at voltage step from −50 mV to + 80 mV (10 mV-increment, 300-msec duration). To exclude the BK_{Ca} current, TEA 1 mmol/L was added in bath solution. Right: summary of normalized amplitude of TEA-sensitive Kv current from CASMCs and MASMCs (*$P < 0.05$). (B) Conductance-voltage relations of steady-state activation and inactivation. The smooth curves were fitted to Boltzmann equation. Half activation voltage ($V_{1/2}$) and slope value (*k*) were 11 ± 2.2 and 18 ± 0.9 mV for MASMCs (open triangle symbol) and 17 ± 1.7 and 16 ± 0.6 mV for CASMCs (filled square symbol). The $V_{1/2}$ and *k* of the steady-state inactivation were −25 ± 3.0 and 7.3 ± 0.4 mV for MASMCs and −35 ± 2.5 and 7.6 ± 0.3 mV for CASMCs, respectively. (C) Inhibition of I_{Kv} by 1 mmol/L 4-AP in MASMCs ($^{\dagger}P < 0.01$). (D) An original trace of D_{in} recording from pressurized MA in response to 1 mmol/L 4-AP. (E) Summary of recorded D_{in} values under 1 mmol/L 4-AP treatment in MA.

curve). Throughout the tested voltages, the density of I_{CaV} (pA/pF) was larger in MASMCs than CASMCs (Fig. 1E).

Next we analyzed the K^+ channel currents, I_{Kv} and I_{BKCa}, using KCl-rich pipette solution. To selectively record I_{Kv}, 5 mmol/L EGTA was included in the pipette solution and 1 mmol/L TEA was added to the bath solution. From −90 mV of holding voltage, step-like depolarizing pulses were applied, which induced outward current from above −40 mV. The density of peak I_{Kv} (pA/pF) was about twofold higher in MASMCs than CASMCs (Fig. 2A). Voltage-dependent steady-state activation and inactivation of I_{Kv} were also analyzed. For the activation kinetics, peak Kv currents at test voltages were converted to conductance (g) and normalized to the

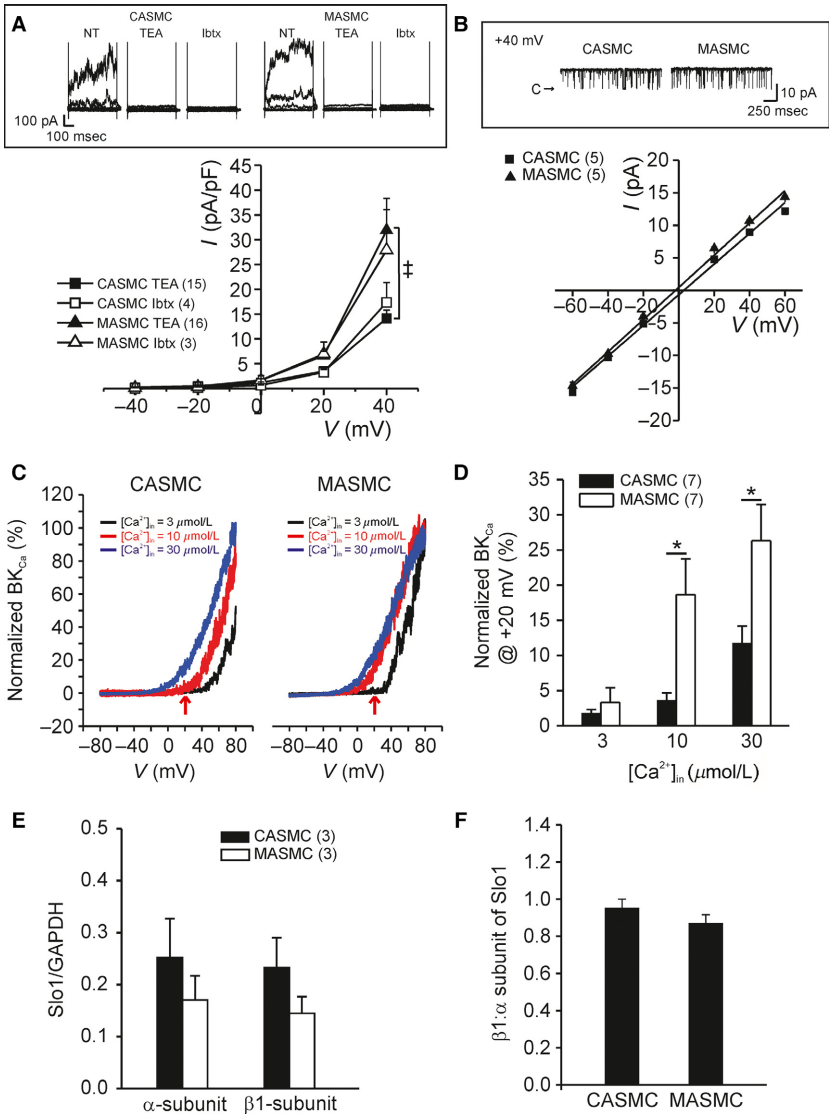

Figure 3. Electrophysiological property of BK_{Ca} channel and qPCR analysis of Slo1α, Sloβ1-subunit from isolated CASMCs and MASMCs. (A) Upper: representative current traces in whole-cell configuration with fixed intracellular Ca^{2+} activity to 1 μmol/L. Outward currents were mostly inhibited by 1 mmol/L TEA and 100 nmol/L iberiotoxin. Lower: summary of TEA-sensitive and iberiotoxin (Ibtx)-sensitive BK_{Ca} current density in CASMCs and MASMCs ($^{\ddagger}P < 0.001$). (B) Upper: representative unitary current recorded at +40 mV in inside-out configuration with intracellular free Ca^{2+} of 1 μmol/L. Lower: unitary current–voltage (I–V) relationship of BK_{Ca} channels in CASMCs and MASMCs. (C) Normalized current–voltage relationship with maximum current at +80 mV in free Ca^{2+} 30 μmol/L concentration. (D) Summary of the normalized BK_{Ca} current at +20 mV in response to a three range of free Ca^{2+} concentrations (3, 10 and 30 μmol/L). (E) Bar graph showing the relative mRNA abundance of Slo1α and Sloβ1 analyzed with $2^{-\Delta\Delta Ct}$ between CASMCs and MASMCs. (F) Ratio of Sloβ1: Slo1α BK_{Ca} subunit mRNA expression between CASMCs and MASMCs.

maximum conductance at +80 mV (g/g_{max}). The conductance to voltage relations were fitted to Boltzmann equation to obtain the half-activation voltages, that were not different between MASMCs and CASMCs (Fig. 2B). For the inactivation kinetics, double-pulse protocol was applied. The peak currents were measured at a 100 msec test voltage of +40 mV after 15 sec preconditioning voltages from −90 to +30 mV. The steady-state inactivation curve was fitted with the Boltzmann equation. The fitted parameters are provided in Figure 2 legend. The analyses revealed that the voltage-dependent inactivation of I_{Kv} occurs at more depolarized ranges in MASMCs than in CASMCs (Fig. 2B). The inactivation kinetics of I_{Kv} suggested that the steady-state conductance of Kv in MASMCs would be higher than CASMCs at the depolarized membrane voltages above the threshold of Kv activation (Fig. 2B).

To investigate the contribution of Kv activity to MT_{MA}, a Kv inhibitor, 4-aminopyridine (4-AP) was applied. The amplitudes of I_{Kv} was decreased to about 50% of control by 1 mmol/L of 4-AP, respectively (Fig. 2C). However, the D_{in} of pressurized MA at 60 mmHg was not significantly affected by the treatment with 1 mmol/L 4-AP (Fig. 2D and E).

Then we analyzed the BK_{Ca} activity to compare between MASMCs and CASMCs. With 1 μmol/L intracellular free Ca^{2+} activity buffered by 10 mmol/L EGTA, the membrane voltage was held at −10 mV to induce the inactivation of Kv. Step-like voltage changes were applied up to +40 mV, which induced outward currents with fluctuating noise. Most of the outward currents were abolished by 1 mmol/L TEA and 100 nmol/L iberiotoxin, relatively selective blockers of BK_{Ca} at this concentration (Fig. 3A, upper panel). The TEA-sensitive and

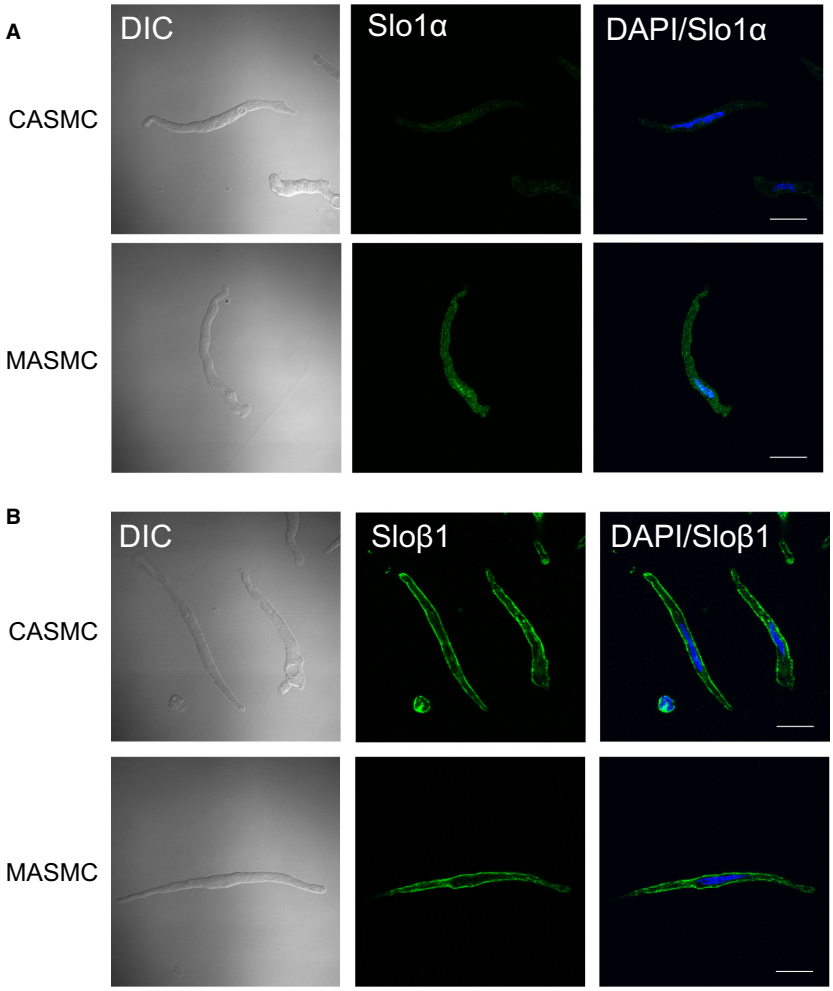

Figure 4. Representative immunofluorescence images of Slo1α- and Sloβ1-subunits in CASMCs and MASMCs. (A–B) Left: differential interference contrast (DIC) image of cells. Middle: staining of Slo1α- or Sloβ1-subunit in green. Right: Overlay with DAPI staining for nucleus (blue). Origianl magnification (×100). Scale bars, 20 μm.

iberiotoxin-sensitive BK_{Ca} currents were significantly higher in MASMCs than in CASMCs (Fig. 3A, lower panel).

Single channel activities of BK_{Ca} were analyzed under the inside-out patch-clamp conditions with 1 μmol/L free Ca^{2+} activity at the cytoplasmic side (Fig. 3B, upper panel). Typical large amplitudes of unitary current with slope conductances around 240 pS were commonly observed in MASMCs and CASMCs (MASMC; 247 $\pm$ 7.5 pS, CASMC; 236 $\pm$ 7.4 pS, Fig. 3B). The Ca^{2+}-dependent activation of BK_{Ca} resides on the sensitization of their voltage-dependent gating property with raised $[Ca^{2+}]_c$ (Cui et al. 2009; Carvalho-de-Souza et al. 2013). Therefore we tested whether the voltage-dependent activation of BK_{Ca} at fixed $[Ca^{2+}]_c$ is different between MASMCs and CASMCs. In the inside-out patches with multiple BK_{Ca}, ramp-like depolarizations from -80 to $+80$ mV were applied with 3, 10 and 30 μmol/L $[Ca^{2+}]_c$ (Fig. 3C). Since the number of BK_{Ca} in the individual membrane patch is variable, the current–voltage relation was normalized to the maximum value at +80 mV with 30 μmol/L $[Ca^{2+}]_c$. The normalized values commonly indicated that the Ca^{2+}-dependent voltage sensitivity of BK_{Ca} is higher in MASMCs than in CASMCs (Fig 3C and D).

Despite the significant difference in the current density and voltage-dependency of BK_{Ca}, α and β1-subunits of BK_{Ca} mRNA levels showed no difference between isolated CASMCs and MASMCs (Fig. 3E and F). To get a clue whether the protein expression of BK_{Ca}, α and β1-subunits is different between MAMSCs and CASMCs, we performed immunofluorescence confocal microcopy. According to the microscopic images, the BK_{Ca} α-subunit specific fluorescence signals (Fig. 4A) in MASMCs seemed to higher than in CASMCs. In contrast, the β1-subunit showed no significant difference (Fig. 4B).

The STOCs reflecting the BK_{Ca} activity triggered by Ca^{2+} sparks were recorded at -20 mV in the whole-cell patch clamp with 0.1 mmol/L EGTA in the pipette solution (Fig. 5A). The number of events, mean peak amplitudes, and averaged areas of STOCs were commonly higher in MASMCs than CASMCs (Fig. 5B–D). The mean peak amplitudes of STOCs (Fig. 5C) were calculated by dividing the sum of event amplitudes by the number of STOCs.

Finally, the contribution of BK_{Ca} activity to the MT was examined in MA and CA pressurized to 60 mmHg. Application of iberiotoxin induced more significant constriction in MA than CA (Fig. 6A). We also investigated the effect of additional structurally different maxi-K channel blocker, TEA. The averaged D_{in} levels, the normalized changes in D_{in} ($\Delta D_{TEA\ or\ Ibtx}/D_{max,0Ca}$), and MT levels with or without 1 mmol/L TEA and 100 nmol/L

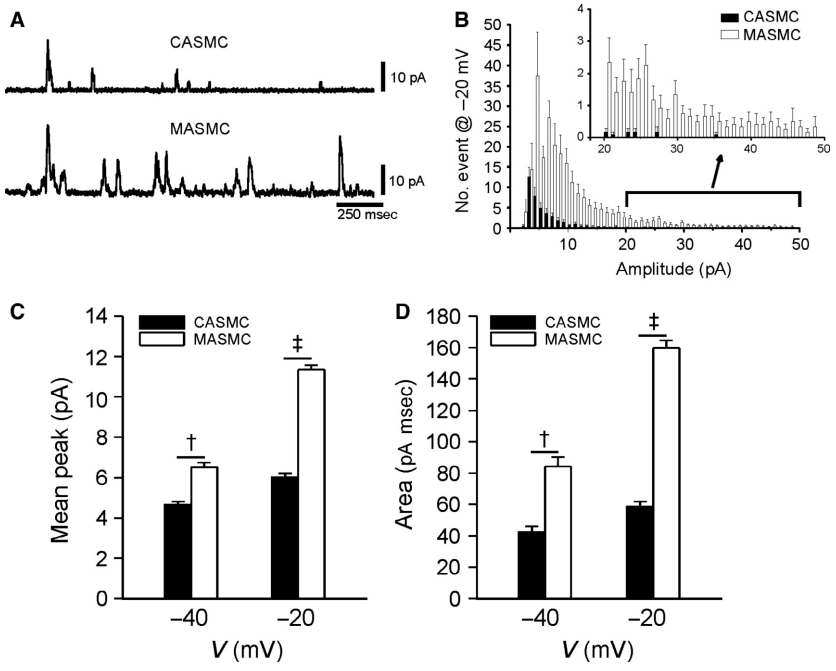

Figure 5. Comparison of STOCs parameters between CASMCs and MASMCs. (A) Representative traces of STOCs detected at -20 mV. STOCs were recorded under whole-cell configuration with low Ca^{2+} buffer (0.1 mmol/L EGTA) in the pipette solution. (B) Summarized amplitude histogram (1 pA bin size) of STOCs recorded at -20 mV during 1-min recordings from 12 cells. (C–D) Summary of STOCs mean peak (C) and area (D) obtained from isolated VSMCs at different holding voltages (-40, -20 mV) ($^{\dagger}P < 0.01$, $^{\ddagger}P < 0.001$).

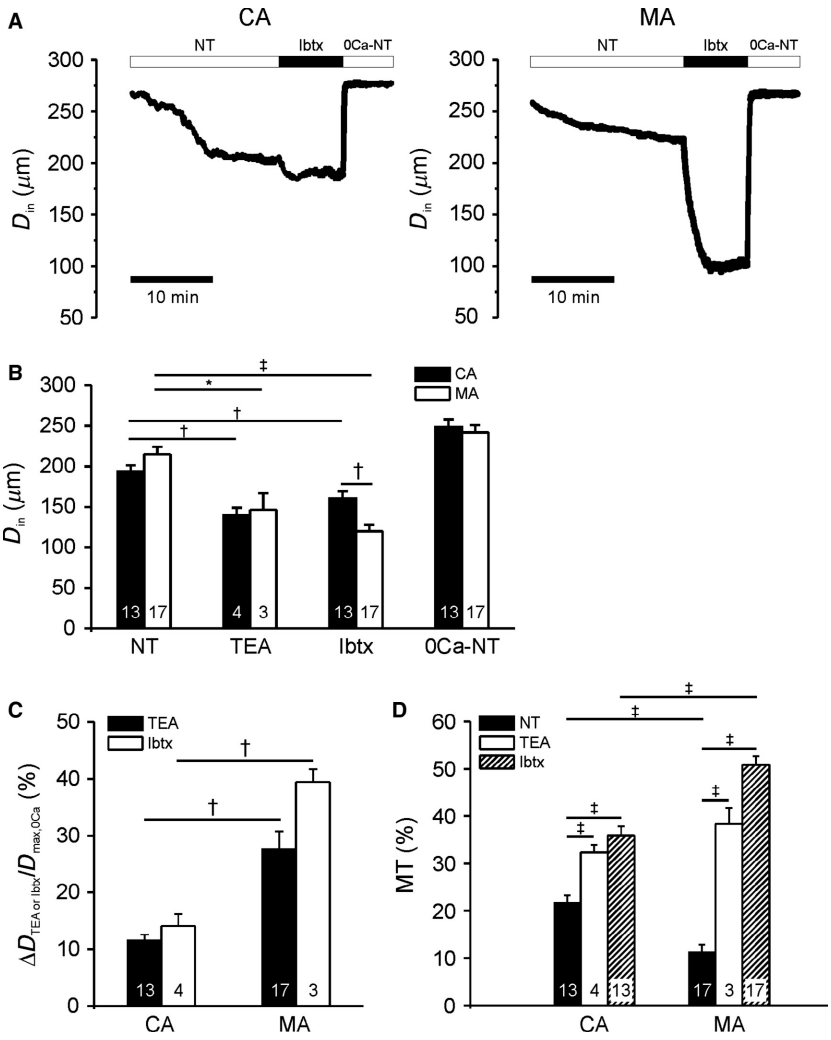

Figure 6. Effects of BK_{Ca} blockers on pressurized CA and MA at 60 mmHg. (A) Representative traces of D_{in} change induced by 100 nmol/L iberiotoxin (Ibtx) from CA (left) and MA (right) at 60 mmHg of P_{lum}. (B) Summary of D_{in} in spontaneous MT in control (NT), with 1 mmol/L TEA, with 100 nmol/L Ibtx and 0Ca-NT conditions (*$P < 0.05$, †$P < 0.01$, ‡$P < 0.001$). (C) Summary of normalized D_{in} changes ($\Delta D_{in}/D_{max,0Ca}$) induced by TEA or Ibtx (†$P < 0.01$). (D) Summary of the MT after the treatment with TEA or Ibtx in comparison with the control MT in NT (‡$P < 0.001$).

iberiotoxin were summarized as bar graphs (Fig. 6B–D). The D_{in} was decreased by TEA and iberiotoxin treatment in CASMCs and MASMCs, which was more prominent at MASMCs.

Discussion

This study showed that MT_{MA} is consistently smaller than MT_{CA} despite the higher amplitudes of I_{CaV} in MASMCs than in CASMCs. Both I_{Kv} and I_{BKCa} were higher in MASMCs than in CASMCs. The pharmacological test with iberiotoxin and TEA suggests that the higher BK_{Ca} activity in MASMCs effectively attenuates the MT_{MA}, most likely through the hyperpolarizing influence. In contrast to our study, a previous report by Chlopicki et al. showed that the sustained phase of MT_{MA} was weakened by BK_{Ca} inhibitor, charybdotoxin (Chlopicki et al. 2001). However, because the K^+ channel blocker would induce membrane depolarization, it is very hard to interpret the paradoxical vasorelaxation reported by Chlopicki et al.

Despite the significant density of I_{Kv}, the application of 4-AP did not change MT_{MA}, indicating relatively small contribution of Kv to the membrane potential of MA under physiological pressure. The I_{Kv} in MASMCs might play significant roles under additional depolarizing influences from vasoactive agonists.

The higher density of I_{BKCa} in both whole-cell and inside-out conditions with fixed $[Ca^{2+}]_c$ strongly suggests higher level of BK_{Ca} expression in the plasma membrane of MASMCs than CASMCs. Additionally, the Ca^{2+}-sensitivity of BK_{Ca} analyzed in inside-out configuration also appeared higher in MASMCs than CASMCs (Fig. 3C and D). Because the unitary slope conductance of BK_{Ca} are not different (Fig. 3B), the α-subunit of BK_{Ca} (Slo1α) seem to be same between MASMCs and CASMCs (Xia et al. 2002).

According to Yang et al., BK_{Ca} activity in rat CASMCs is higher than skeletal arterial myocytes that was ascribed to the higher ratio of β1-subunit over α-subunit of Slo1 (Yang et al. 2009, 2013). In our hands, the qPCR analysis did not reveal a difference of Slo1α and β1 subunits between MASMCs and CASMCs (Fig. 3E and F). Unfortunately we could not directly analyze the protein amounts between the small resistance MAs and CAs due to the tiny amounts of myocytes available after the enzymatic single cell isolation. Although we could not conduct immunoblot assays, we performed immunofluorescence confocal microscopy to compare the expression levels of BK_{Ca} subunits. Although the confocal images require careful interpretation in terms of the protein expression levels, the experimental results suggest that Slo1α expression appeared higher in MASMCs than CASMCs (Fig. 4A). In both cell types, Sloβ1 signal was more prominently observed than the Slo1α, while no significant difference between MASMCs and CASMCs (Fig. 4B). Taken together, the functional difference of BK_{Ca} current density might be ascribed to the differential expression of Slo1α. Also, an unidentified difference in channel modulatory factors might underlie the higher Ca^{2+}-sensitivity of BK_{Ca} in MASMCs, which requires further investigation.

The more prominent STOCs in MASMCs (Fig. 5) might be due to the putatively higher Ca^{2+}-sensitivity of BK_{Ca} and more frequent generation of Ca^{2+} sparks in MASMCs. Because the Ca^{2+} sparks can be triggered by flickering activation of CaV, the higher density of CaV in MASMCs might also contribute to the more frequent STOCs. In contrast to the global $[Ca^{2+}]_c$ increase, Ca^{2+} sparks negatively regulate contraction of arterial smooth muscle (Jaggar et al. 1998). The physiological role of STOCs became evident from the case of impaired coupling between STOC and Ca^{2+} spark coupling in the arterial myocytes of diabetic rat model (Rueda et al. 2013). A rigorous comparison between STOCs with Ca^{2+} sparks using confocal microscopy combined with patch-clamp study might provide more clear evidence of the putative differential STOCs/Ca^{2+} spark coupling between different arteries.

Physiological implication of the different MR and ion channel activities

A previous study of intestinal microcirculation has shown that the microvilli blood flow is effectively autoregulated while less effective in the muscular layer (Davis and Gore 1985). Although the autoregulation of intestinal blood flow is mainly observed at the submucosal arterioles, due to the large volume of intestinal tissue to be perfused, the blood flow through the MA branches would be relatively higher than that of the CA with similar diameter. In this respect, the weak MR_{MA} would be physiologically relevant, and the higher activity of BK_{Ca} would be a compensatory property to keep the low MT_{MA} despite the higher I_{CaV}. The weak MT_{MA} also implies intrinsically low resistance without vasoactive signals. On the other hand, the low resistance of MA might be more beneficial to effectively redirect the intestinal blood flow for the recruitment under 'fight and flight' conditions. Under such conditions, the higher density of I_{Kv} might play a role to counterbalance the excessive vasoconstriction of MA (Fig. 2A and B).

In comparison with the other systemic arteries, sympathetic regulation is minimized in the cerebral resistance arteries, and the MT-dependent autoregulation seems to be the critical mechanism for the constant cerebral blood flow. The marked MT_{CA} coupled with their parallel arrangement would promote regional regulation of flow with minimal overall changes in blood volume. Also, according to LaPlace's law, the myogenic constriction would effectively decrease the wall tension and thus reduces the stimulus for further constriction. Thus, the more sensitive MT_{CA} might enable to maintain a lower wall tension in CA than the similar sizes of MA. Previously, the mechanism underlying such difference may be related to a higher I_{CaV} in CASMCs (Asano et al. 1993). However, our present study showed that the differential activity of K^+ channels in VSMC might be more critical factor to determine the level of MT.

In summary, our study indicate that MA contain an intrinsic capacity of potent MT that is veiled by higher BK_{Ca} activities. The differential patterns of ion channel currents may provide variability in MT and underlying membrane voltages in the arteries suppling heterogeneous tissues and organs. Physiological and pharmacological modulation of BK_{Ca} would be an effective manner to regulate the intestinal blood flow.

Conflict of Interest

No conflicts of interest, financial or otherwise, are declared by the authors.

References

Asano, M., K. Masuzawa-Ito, T. Matsuda, Y. Suzuki, H. Oyama, M. Shibuya, et al. 1993. Functional role of charybdotoxin-sensitive K^+ channels in the resting state of cerebral, coronary and mesenteric arteries of the dog. J. Pharmacol. Exp. Ther. 267:1277–1285.

Baek, E. B., C. Jin, S. J. Park, K. S. Park, H. Y. Yoo, J. H. Jeon, et al. 2010. Differential recruitment of mechanisms for myogenic responses according to luminal pressure and arterial types. Pflugers Arch. 460:19–29.

Benham, C. D., and T. B. Bolton. 1986. Spontaneous transient outward currents in single visceral and vascular smooth muscle cells of the rabbit. J. Physiol. 381:385–406.

Bolton, T. B., and Y. Imaizumi. 1996. Spontaneous transient outward currents in smooth muscle cells. Cell Calcium 20:141–152.

Carvalho-de-Souza, J. L., W. A. Varanda, R. C. Tostes, and A. Z. Chignalia. 2013. BK Channels in Cardiovascular Diseases and Aging. Aging Dis. 4:38–49.

Chlopicki, S., H. Nilsson, and M. J. Mulvany. 2001. Initial and sustained phases of myogenic response of rat mesenteric small arteries. Am. J. Physiol. Heart Circ. Physiol. 281: H2176–H2183.

Cipolla, M. J., J. Sweet, S. L. Chan, M. J. Tavares, N. Gokina, and J. E. Brayden. 2014. Increased pressure-induced tone in rat parenchymal arterioles vs. middle cerebral arteries: role of ion channels and calcium sensitivity. J. Appl. Physiol. 117:53–59.

Cui, J., H. Yang, and U. S. Lee. 2009. Molecular mechanisms of BK channel activation. Cell. Mol. Life Sci. 66:852–875.

Davis, M. J., and R. W. Gore. 1985. Capillary pressures in rat intestinal muscle and mucosal villi during venous pressure elevation. Am. J. Physiol. 249:H174–H187.

Enouri, S., G. Monteith, and R. Johnson. 2011. Characteristics of myogenic reactivity in isolated rat mesenteric veins. Am. J. Physiol. Regul. Integr. Comp. Physiol. 300:R470–R478.

Harder, D. R. 1984. Pressure-dependent membrane depolarization in cat middle cerebral artery. Circ. Res. 55:197–202.

Hill, M. A., M. J. Davis, G. A. Meininger, S. J. Potocnik, and T. V. Murphy. 2006. Arteriolar myogenic signalling mechanisms: implications for local vascular function. Clin. Hemorheol. Microcirc. 34:67–79.

Hill, M. A., Y. Yang, S. R. Ella, M. J. Davis, and A. P. Braun. 2010. Large conductance, Ca^{2+}-activated K^+ channels (BKCa) and arteriolar myogenic signaling. FEBS Lett. 584:2033–2042.

Hu, X. Q., and L. Zhang. 2012. Function and regulation of large conductance Ca^{2+}-activated K^+ channel in vascular smooth muscle cells. Drug Discov. Today 17:974–987.

Isenberg, G., and U. Klockner. 1982. Calcium tolerant ventricular myocytes prepared by preincubation in a "KB medium". Pflugers Arch. 395:6–18.

Jaggar, J. H., G. C. Wellman, T. J. Heppner, V. A. Porter, G. J. Perez, M. Gollasch, et al. 1998. Ca^{2+} channels, ryanodine receptors and Ca^{2+}-activated K^+ channels: a functional unit for regulating arterial tone. Acta Physiol. Scand. 164:577–587.

Jin, C. Z., H. S. Kim, E. Y. Seo, D. H. Shin, K. S. Park, Y. S. Chun, et al. 2011. Exercise training increases inwardly rectifying K^+ current and augments K^+-mediated vasodilatation in deep femoral artery of rats. Cardiovasc. Res. 91:142–150.

Johnson, P. C. 1977. Landis Award Lecture. The myogenic response and the microcirculation. Microvasc. Res. 13:1–18.

Kotecha, N., and M. A. Hill. 2005. Myogenic contraction in rat skeletal muscle arterioles: smooth muscle membrane potential and Ca^{2+} signaling. Am. J. Physiol. Heart Circ. Physiol. 289:H1326–H1334.

Lagaud, G. J., P. L. Skarsgard, I. Laher, and C. van Breemen. 1999. Heterogeneity of endothelium-dependent vasodilation in pressurized cerebral and small mesenteric resistance arteries of the rat. J. Pharmacol. Exp. Ther. 290:832–839.

Lagaud, G., N. Gaudreault, E. D. Moore, C. Van Breemen, and I. Laher. 2002. Pressure-dependent myogenic constriction of cerebral arteries occurs independently of voltage-dependent activation. Am. J. Physiol. Heart Circ. Physiol. 283:H2187–H2195.

Lundgren, O. 1989. Autoregulation of intestinal blood flow: physiology and pathophysiology. J. Hypertens. Suppl. 7: S79–S84.

Mathewson, A. M., and W. R. Dunn. 2014. A comparison of responses to raised extracellular potassium and endothelium-derived hyperpolarizing factor (EDHF) in rat pressurised mesenteric arteries. PLoS ONE 9:e111977.

Pérez, G. J., A. D. Bonev, J. B. Patlak, and M. T. Nelson. 1999. Functional coupling of ryanodine receptors to K_{Ca} channels in smooth muscle cells from rat cerebral arteries. J. Gen. Physiol. 113:229–238.

Rueda, A., M. Fernández-Velasco, J. P. Benitah, and A. M. Gómez. 2013. Abnormal Ca^{2+} spark/STOC coupling in cerebral artery smooth muscle cells of obese type 2 diabetic mice. PLoS ONE 8:e53321.

Smith, P. D., S. E. Brett, K. D. Luykenaar, S. L. Sandow, S. P. Marrelli, E. J. Vigmond, et al. 2008. KIR channels function as electrical amplifiers in rat vascular smooth muscle. J. Physiol. 586:1147–1160.

Sonkusare, S. K., T. Dalsgaard, A. D. Bonev, and M. T. Nelson. 2016. Inward rectifier potassium (Kir2.1) channels as end-stage boosters of endothelium-dependent vasodilators. J. Physiol. 594:3271–3285.

Standen, N. B., and J. M. Quayle. 1998. K^+ channel modulation in arterial smooth muscle. Acta Physiol. Scand. 164:549–557.

Sun, D., E. J. Messina, G. Kaley, and A. Koller. 1992. Characteristics and origin of myogenic response in isolated mesenteric arterioles. Am. J. Physiol. 263:H1486–H1491.

VanBavel, E., M. J. Giezeman, T. Mooij, and J. A. Spaan. 1991. Influence of pressure alterations on tone and vasomotion of isolated mesenteric small arteries of the rat. J. Physiol. 436:371–383.

Wesselman, J. P., E. VanBavel, M. Pfaffendorf, and J. A. Spaan. 1996. Voltage-operated calcium channels are essential for the myogenic responsiveness of cannulated rat mesenteric small arteries. J. Vasc. Res. 33:32–41.

Xia, X. M., X. Zeng, and C. J. Lingle. 2002. Multiple regulatory sites in large-conductance calcium-activated potassium channels. Nature 418:880–884.

Yang, Y., T. V. Murphy, S. R. Ella, T. H. Grayson, R. Haddock, Y. T. Hwang, et al. 2009. Heterogeneity in function of small artery smooth muscle BKCa: involvement of the beta1-subunit. J. Physiol. 587: 3025–3044.

Yang, Y., Y. Sohma, Z. Nourian, S. R. Ella, M. Li, A. Stupica, et al. 2013. Mechanisms underlying regional differences in the Ca^{2+} sensitivity of BK(Ca) current in arteriolar smooth muscle. J. Physiol. 591:1277–1293.